

A Theoretical Model for Resonant Frequency and Radiation Pattern on Rectangular Microstrip Patch Antenna on Liquid Crystal Substrate

Tae-Wan Kim¹, Jun-Sung Park, and Seong-Ook Park, *Senior Member, IEEE*

Abstract—This paper presents a theoretical model of the rectangular-shaped microstrip patch antennas on liquid crystal (LC) substrates in order to accurately derive the resonant frequencies and radiation performances. The model is based on the solution of the mode matching about an LC loaded cavity. The calculation results of the theoretical model are compared with the experiment and simulation results. The discrepancy between calculation and simulation results is merely 2.7%. In addition, a tuning mechanism of the patch antenna on the LC substrate is verified depending on the strength of a biasing voltage. The calculated results of the theoretical model indicate that the resonant frequency is shifted toward lower direction and 3-dB beamwidth of radiation pattern increases as the bias voltage increases. Although the calculated maximum directivity decreases with the increment of voltage, the realized gain increases due to the radiation efficiency of the antenna.

Index Terms—Liquid crystal (LC) devices, microstrip antennas, modeling, reconfigurable antennas.

I. INTRODUCTION

WITH the development of wireless communication, the study about microstrip patch antenna has been rapidly developed and published, because the patch antenna has attractive features. However, the narrow bandwidth characteristic of patch antenna became the main problem for practical use. To overcome the disadvantage, the reconfigurable patch antenna based on the liquid crystal (LC) substrate is suggested because LC has anisotropic dielectric constant, birefringence, and ability to change the dielectric properties depending on the dc bias voltage [1], [2].

Recently, experiment and simulation results of LC-based patch antenna have been introduced in [3]–[9]. A reconfigurable patch antenna based on the E-7 type LC substrates was proposed in [3]. They obtained the measured and simulation results using the effective dielectric properties. Martin *et al.* [4], [5] introduced the reconfigurable and

miniaturized antennas using two-kinds of LC materials. They acquired the 3% tuning ability and the 39% miniaturization. By using the anisotropic and alterable features of the LC, the LC-based patch antenna was analyzed from the simulation results [6], [8].

Unfortunately, although some experiment and simulation results were studied, it is very important and difficult to explain theoretically the tuning mechanism of the antenna with such a bias direction. To analyze the performance of the antenna on the anisotropic substrate, the minimum number of numerical and simulation models were proposed in [10]–[12] and [17]–[19]. Boutout *et al.* [11] proposed the statistic equation of the patch antenna on the anisotropic material based on the well-known Galerkin procedure of the moment method. However, the statistic equation did not contain the influence of the substrate thickness. To derive the accurate simulation results, some research team [12] introduced the permittivity tensor model of the antenna based on the solution of Poisson's equation coupled to a nonlinear partial differential equation describing the orientation of the directors in a nonhomogeneous electric field. Perez-Palomino *et al.* [17] also introduced the electromagnetic modeling for an accurate analysis of reconfigurable reflect-array cells based on the LC. By considering the nonuniform bias fields, they obtained the accurate simulation results.

Although the LC-based patch antenna was analyzed by the numerical method, the practical and simple theoretical model is required in order to design and use the antenna for practical purpose. However, in the patch antenna on the LC substrate case, only a theoretical model of the isotropic case was used by applying the effective permittivity instead of the anisotropic properties [8], [9]. The isotropic theoretical model was not able to analyze the LC-based patch antenna, precisely. Therefore, a new formula containing the anisotropic property of the LC is required for an accurate design of the antenna and determines the resonant frequencies as well as the radiation performances of the patch antenna on the LC substrate.

In this paper, we propose an analytical model to predict the frequency response and radiation performances of the patch antenna on the LC substrate. The model is based on the solutions of mode matching about an anisotropic medium loaded cavity. A formula to calculate the resonant frequency of the patch antenna for the TM modes is presented, which considers the effective dimension considering fringing effect.

Manuscript received January 11, 2018; revised May 14, 2018; accepted May 31, 2018. Date of publication July 2, 2018; date of current version August 31, 2018. This work was supported by the Basic Science Research Program through the National Research Foundation of Korea by the Ministry of Science, ICT & Future Planning under Grant 2016R1A2B4010918. (Corresponding author: Tae-Wan Kim.)

The authors are with the Department of Electrical Engineering, Korea Advanced Institute of Science and Technology, Daejeon 305-732, South Korea (e-mail: gold427@kaist.ac.kr; kirasnip@kaist.ac.kr; sopark@ee.kaist.ac.kr).

Color versions of one or more of the figures in this paper are available online at <http://ieeexplore.ieee.org>.

Digital Object Identifier 10.1109/TAP.2018.2851304

Considering the Fringing effect, the effective dimensions of patch antenna are larger than that of the practical dimensions of the patch antenna. In the case of dominant mode, effective dimension, W_e and L_e , may be represented as follows [15]:

$$\begin{cases} W_e = W \\ L_e = L + 2\Delta L = L[1 + \delta(L)]\frac{\sqrt{\varepsilon_e L \varepsilon_e W}}{\varepsilon_z} \end{cases} \quad (8)$$

where

$$\begin{aligned} \delta(L) &= \frac{h_{\text{eff}}}{L} \left\{ 0.882 + \frac{0.162(\varepsilon_z - 1)}{\varepsilon_z^2} \right. \\ &\quad \left. + \frac{\varepsilon_z + 1}{\pi \varepsilon_z} \left[0.758 + \ln \left(\frac{L}{h_{\text{eff}}} + 1.88 \right) \right] \right\} \\ \varepsilon_{eL,eW} &= \frac{1}{2} \left[(\varepsilon_z + 1) + (\varepsilon_z - 1) \left(1 + \frac{10h_{\text{eff}}}{L, W} \right)^{-0.5} \right] \end{aligned}$$

$\varepsilon_{eL,eW}$ is the substrate effective permittivity [16] as a function of patch length L and width W .

Finally, using (7) and (8), the resonant frequencies for the cavity are given by

$$f_{mnl} = \frac{1}{2\pi\sqrt{\varepsilon_z}} \sqrt{\left(\frac{m\pi}{W_e}\right)^2 + \left(\frac{n\pi}{L_e}\right)^2 + \left(\frac{l\pi}{h_e}\right)^2}. \quad (9)$$

Using (9), we can estimate not only a dominant mode but also resonant frequencies of the higher order modes of the patch antenna. Also, we can conclude that the resonant frequency is mainly influenced only by the vertical permittivity tensor component at resonance direction. For example, the resonance mode in the x - or y -direction is affected by the change of ε_z . In addition, the z -direction resonance mode is influenced by the change of ε_{\perp} . In most case of the microstrip patch antenna on the LC substrate, the parallel tensor component, ε_z , affects resonant frequency predominantly since the z -direction resonance of patch antenna does not exist at TE mode. Boutout *et al.* [11] verified these results by statistic equation and approximation formula approach with the limit of small substrate thickness. On the assumption that substrate thickness h is extremely small, the anisotropic substrate behaves like the isotropic substrate with relative permittivity equal to ε_z . Therefore, the proposed formula (9) reflects the results of [11] well. In addition, the effect of the substrate thickness can be demonstrated by the proposed method. The transverse permittivity tensor component ε_{\perp} affects the variation of the resonant frequency of dominant mode, marginally, because the effective height h_e appears on a formula by ε_{\perp} and ε_z as shown in (6). When the substrate becomes thick, the impact of ε_{\perp} on the resonant frequency increases because TE propagation waves are also radiated as well as TM waves.

B. Radiation Performance

The fields on the side of the rectangular patch are replaced with equivalent current sources. The equation about equivalent current sources from [13] is as follows:

$$\vec{J}_s = \hat{n} \times \vec{H}, \quad \vec{M}_s = \vec{E} \times \hat{n} \quad (10)$$

where \hat{n} is a unit normal pointing outward from the surface.

For the special case of a rectangular patch antenna, electric surface current source \vec{J}_s is zero and considers only magnetic surface current source \vec{M}_s because there are no H-fields on the surface on the assumption of magnetic wall. Generally, the patch antenna can be regarded as an antenna system equivalent to the two-slot model. The radiation pattern is determined by multiplying the radiated field of a single slot by an array factor corresponding to the arrangement of a two-slot array. Based on the electric field components inside the anisotropic material that are defined from (3) and (5), the total radiation field in the E-plane of a rectangular microstrip antenna element operating in the quasi-TM_{0m0} mode is given in [15] as

$$E_{\theta}(\theta)|_{\phi=0} = -jV_0 W k_0 \left(\frac{e^{-jk_0 R}}{4\pi R} \right) F_E(\theta) \quad (11)$$

where

$$F_E(\theta) = \sin\left(\frac{k_0 h_e}{2} \sin\theta\right) \left(\frac{k_0 h_e}{2} \sin\theta\right)^{-1} \text{AF}$$

with

$$\text{AF} = \begin{cases} \cos\left(\frac{k_0 L_e}{2} \sin\theta\right) & \text{for } m = \text{odd order,} \\ j \sin\left(\frac{k_0 L_e}{2} \sin\theta\right) & \text{for } m = \text{even order.} \end{cases}$$

For the H-plane

$$E_{\phi}(\theta)|_{\phi=\pi/2} = -jV_0 W k_0 \left(\frac{e^{-jk_0 R}}{4\pi R} \right) F_H(\theta) \quad (12)$$

where

$$F_H(\theta) = \sin\left(\frac{k_0 W_e}{2} \sin\theta\right) \left(\frac{k_0 W_e}{2} \sin\theta\right)^{-1} \cos(\theta) \quad \text{for } m = \text{odd order}$$

where V_0 is the voltage across the slot and R , θ , and ϕ are the spherical coordinates defined as Fig. 1. When m is even order, $F_H(\theta)$ vanishes, theoretically, and the radiation pattern of the E-plane only can be obtained. The maximum directivity using (11) and (12) is written by

$$D_0 = \frac{4\pi U}{P_{\text{rad}}} = 4\pi \frac{F(\theta, \phi)|_{\text{max}}}{\int_0^{2\pi} \int_0^{\pi} F(\theta, \phi) \sin\theta d\theta d\phi} \quad (13)$$

where

$$F(\theta, \phi) = |E_{\phi}(\theta, \phi)|^2 + |E_{\theta}(\theta, \phi)|^2.$$

Maximum gain is expressed as

$$G_0 = \eta D_0 \quad (14)$$

where η is the radiation efficiency. The radiation efficiency can be affected by various factors such as the antenna-matching problem and material loss.

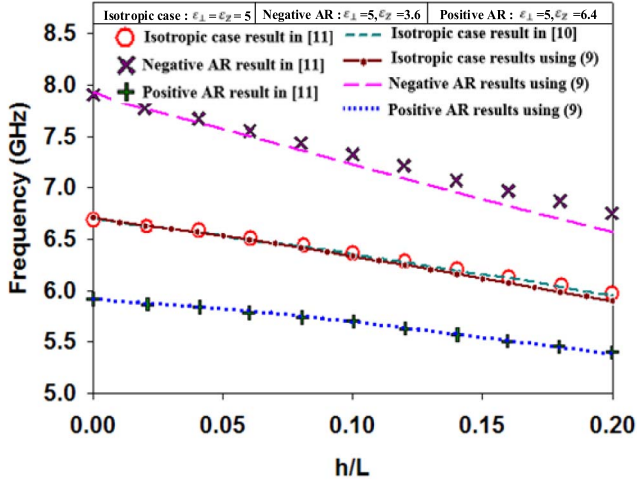


Fig. 2. Resonant frequency as function of substrate thickness when ε_z changed.

III. ANALYSIS OF RESONANT FREQUENCY

The effects of uniaxial anisotropy on the resonant frequency are determined as a function of anisotropy ratio ($AR = \varepsilon_{\perp}/\varepsilon_z$). When the value of ε_{\perp} is equal to that of ε_z , AR is 1 as in the isotropic case. The AR that is above 1 is defined as negative uniaxial anisotropy, and the AR that is less than 1 is called as positive uniaxial anisotropy. In the LC case, AR is negative at no bias condition. When the voltage increases, AR becomes 1 as in the isotropic case at certain bias and is positive at full-saturated state due to the variable characteristic of LC.

To analyze the effect of permittivity tensor components on resonant frequency, the dominant mode is calculated by changing the values of the permittivity tensor components. The area ($W \times L$) of the rectangular patch antenna is 15×10 mm. In addition, the accuracy of our calculation results is verified by comparing with results of [11] that introduced the numerical calculation results of the patch antenna on the uniaxial substrate. The calculated results of the quasi- TM_{010} mode of the patch antenna against normalized substrate thickness are shown in Figs. 2 and 3, where isotropic, negative uniaxial anisotropic, and positive uniaxial anisotropic substrates are considered. Fig. 2 shows the influence of AR by changing ε_z and while maintaining ε_{\perp} . When ε_z increases, the resonant frequency decreases. As mentioned in Section II, the tensor component ε_z influences the resonant frequency significantly, because the quasi- TM_{010} mode resonates at the y -axis direction. However, as the height of the substrate increases, the discrepancy of the resonant frequencies between the positive AR case and negative AR case reduces, although the effect of ε_z still remains. The calculated results of the proposed cavity model match the numerical results of [11] well. In addition, our calculated results are in a good agreement with the calculated results of the isotropic case [10]. With increasing height of the substrate, the error of calculated results of the negative uniaxial substrate case compared with [11] increases and maximum error is 2.8%. One of the reasons for this discrepancy is the ambiguity of (8) because the effective dimensions of patch

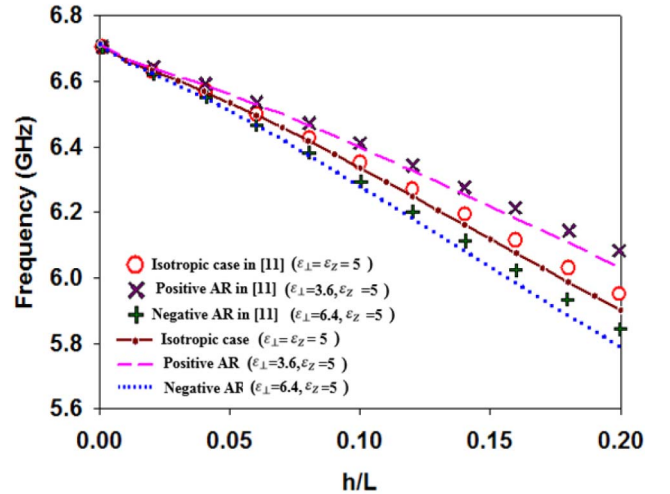


Fig. 3. Resonant frequency as function of substrate thickness when ε_{\perp} changed.

antenna will be changed slightly, depending on the frequency region. Nevertheless, the reasonable results are achieved using the proposed method since the error is very slight and the tendency corresponds to [11] well.

Fig. 3 shows the frequency shifts against substrate thickness when ε_{\perp} changes and ε_z remains constantly. The influence of ε_{\perp} on the resonant frequency is insignificant. However, as the height of the substrate increases, the discrepancy of resonant frequencies between the positive AR and negative AR increases at certain substrate thickness. Nevertheless, the discrepancy at $h/L = 0.2$ is less than 5%. Therefore, these influences are trivial and tend to be neglected for lower substrate thickness. The proposed results, in common with Fig. 2, are in excellent agreement with the results of [11]. Although the discrepancy between the results of proposed model and results of [11] also exists, the discrepancy is merely under 1%, which results from the ambiguity of (8). The effect of ε_{\perp} and height of substrate on resonant frequency cannot be verified by statistic equation of [11], because the equation assumed that the height of substrate is almost zero. In contrast, according to our model, the results of effect of ε_{\perp} and height of substrate to resonant frequency can be successfully verified.

There have been many experiments about the rectangular patch antenna on the LC substrate in [3]–[7]. Typically, the experimental results by Liu and Langley [3] were analyzed by the proposed model. The relative perpendicular and parallel permittivity components, ε_{\perp} and ε_z , are 3.17 and 2.72, respectively, which were the experimental data at 30 GHz in [2] and [1], respectively. Similarly, the corresponding losses, $\tan\delta_{\perp}$ and $\tan\delta_z$, are 0.02 and 0.12, respectively. Based on the given physical dimensions in [3] and measured material parameters, the resonant frequencies from (9) were calculated for various voltage strengths that is varied between 0 and 10 V, as shown in Fig. 4. As expected, the resonant frequencies are tuned according to the voltage. As the strength of the bias voltage increases, the ε_z increases while ε_{\perp} decreases. Therefore, by increasing the voltage, the dominant mode shifts

TABLE I
SUMMARY OF RESULTS OF REPORTED RESULTS AND PROPOSED RESULTS OF RESONANT FREQUENCIES DEPENDING ON VOLTAGE BIAS

	LC material	Measurement Results			Simulation Results			Calculation Results using this Approach		
		No Bias (f_1 GHz)	Saturation Bias (f_2 GHz)	Tunable range ($\Delta f = f_2 - f_1$ GHz)	No Bias (f_1 GHz)	Saturation Bias (f_2 GHz)	Tunable range ($\Delta f = f_2 - f_1$ GHz)	No Bias (f_1 GHz)	Saturation Bias (f_2 GHz)	Tunable range ($\Delta f = f_2 - f_1$ GHz)
[3]	E7	5.65	5.45	0.2	5.76	5.34	0.42	5.75	5.368	0.382
[4]	K15	4.74	4.6	0.14	4.36	4.22	0.14	4.2386	4.1131	0.126
[5]	BL037	4.57	4.33	0.24	4.65	4.44	0.21	4.537	4.3211	0.216
[6]	K15	-	-	-	28	27.25	0.75	27.836	27.01	0.826
[7]	GT3-23001	2.95	2.69	0.26	2.95	2.69	0.26	3.02	2.7	0.32

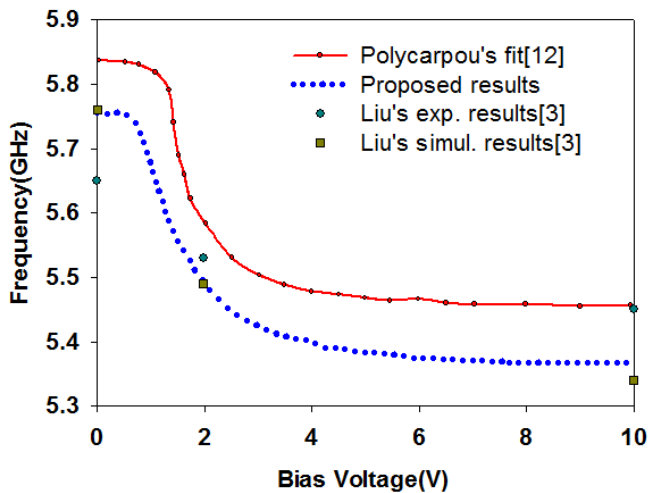


Fig. 4. Antenna resonant frequency versus bias voltage.

to the lower frequencies. The calculated results of the proposed model depending on the various bias conditions highly agree with the measured results of [3]. However, some discrepancies exist. The errors between measured results and calculated results at 0 and 10 V are 1.5% and 1.8%, respectively. In addition, the measured tuning range is smaller than the calculated one. The discrepancies between the measured and calculated results attribute to the fabrication tolerance, such as the air gap between the LC substrate and patch antenna. The simulation results of [3] that are ideal condition correspond to the calculated results well. The maximum error between simulation results and calculated results is less than 0.1%. The simulation results of [12] that attempted to analyze the antenna by using the numerical model are shown in Fig. 4. Although the resonant frequency at certain bias condition is different, the tendency of calculated results of the proposed model depending on the strength of bias highly corresponds to the numerical results of [12]. In addition, the calculated results of the proposed model are more accurate than the simulation results in [12] compared with Liu's study [3].

Table I summarizes the experiment results and simulation results of the rectangular patch antenna on the LC substrate in the past studies [3]–[7] and calculated results of the proposed model. Based on the given antenna dimension and material properties from each paper [1], [2], [14], the theoretical

model (9) is calculated. The calculated values of the resonant frequency are in excellent agreement with the reported measured and simulation results. The error between the measured values and theoretical resonant frequencies occurred fairly much, arising from 0.7% to 10.5%. As mentioned, the error arises due to fabrication tolerance. The differences between reported simulation results and calculated theoretical results of resonant frequency are only less than 2.78%. Consequently, it is verified that the proposed model is reasonable enough to be an established method to find out the resonant frequency of the LC patch antenna.

IV. ANALYSIS OF RADIATION PERFORMANCE

Radiation performances that are radiation pattern, directivity, radiation efficiency, and realized gain of antenna are strongly affected by substrate properties. Radiation efficiency and realized gain are affected by not only expectable causes (substrate loss and conductor loss) but also by unexpected factors (matching problem and fabrication error). In other words, the radiation efficiency and realized gain cannot be predicted with complete accuracy due to unexpected variables. On the other hand, the normalized radiation pattern and directivity can be derived by solving the proposed formula from (11) to (13).

When the patch size is 20×15 mm ($W \times L$) and height of substrate is 0.51 mm, the calculated results of the normalized radiation pattern depending on the variable uniaxial properties can be shown in Fig. 5. There are two distinct characteristics to concern. First, the normalized radiation pattern is not strongly influenced by perpendicular tensor component ϵ_{\perp} . The characteristic can be seen in both E-plane and H-plane. In addition, when the value of ϵ_z increases, the 3-dB beamwidth of radiation patterns increases. The influence of ϵ_z is stronger in the E-plane than in the H-plane. Figs. 6 and 7 show the higher order mode TM_{020} and TM_{030} , respectively. In TM_{020} mode, the null point is generated at $\theta = 0^\circ$ because the two radiating slots have the same magnitude but opposite phase. Fig. 7 shows the effect of uniaxial properties of LC on the radiation pattern of TM_{030} mode. When ϵ_z is low ($\epsilon_z = 1.5$ and 3), the E-plane contains sidelobe. As shown in Fig. 7(a), the sidelobe level is reduced with increasing ϵ_z . Furthermore, when ϵ_z is 5, the side lobes are vanished at the E-plane. In other words, the sidelobe of TM_{030} mode can be adjusted by ϵ_z . Although the sidelobe increases and main lobe decreases

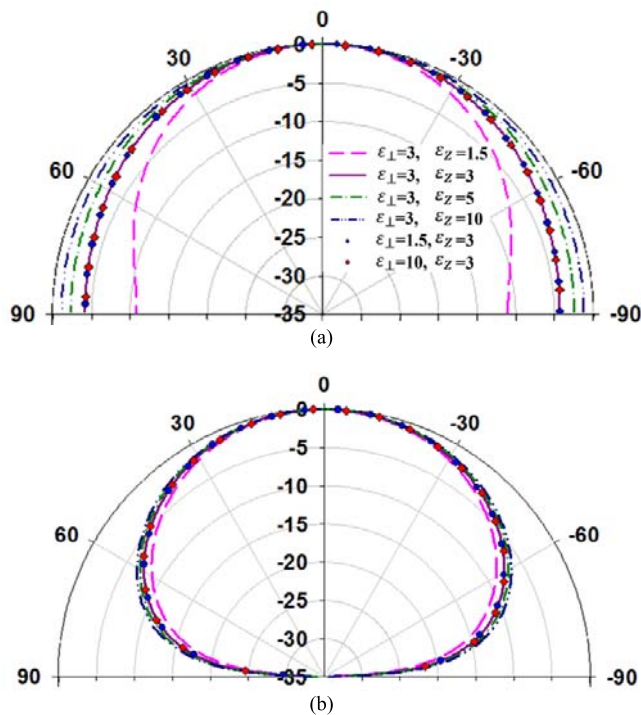


Fig. 5. Theoretical normalized radiation patterns as function of anisotropic permittivity of LC. (a) E-plane. (b) H-plane.

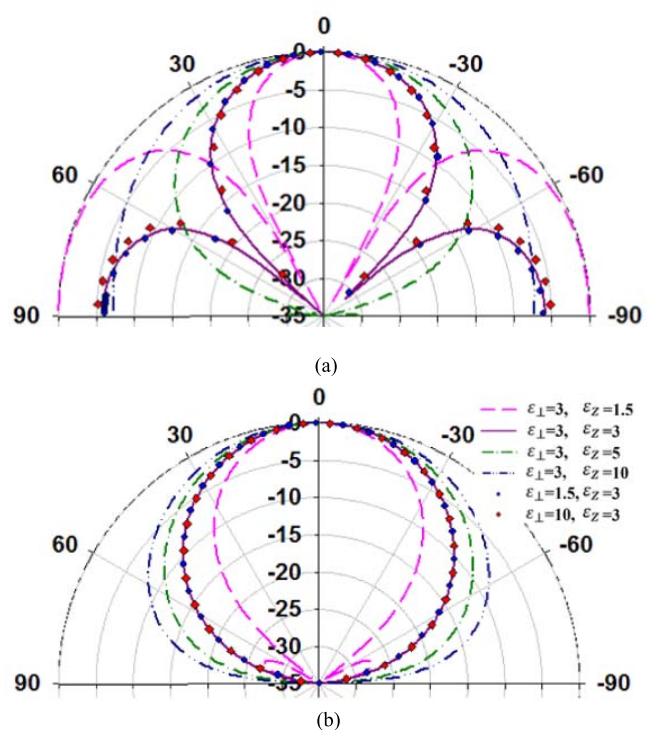


Fig. 7. Theoretical normalized radiation patterns of TM_{030} as function of anisotropic permittivity of LC. (a) E-plane. (b) H-plane.

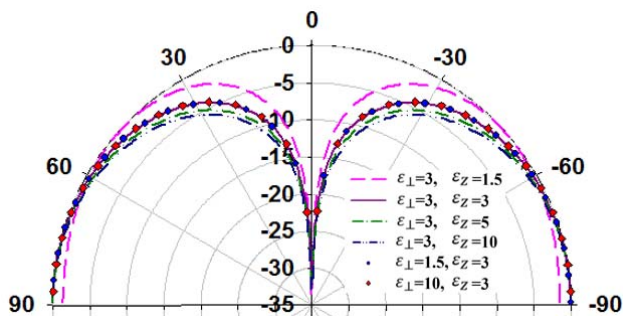


Fig. 6. Theoretical normalized radiation patterns of E-plane of TM_{020} as function of anisotropic permittivity of LC.

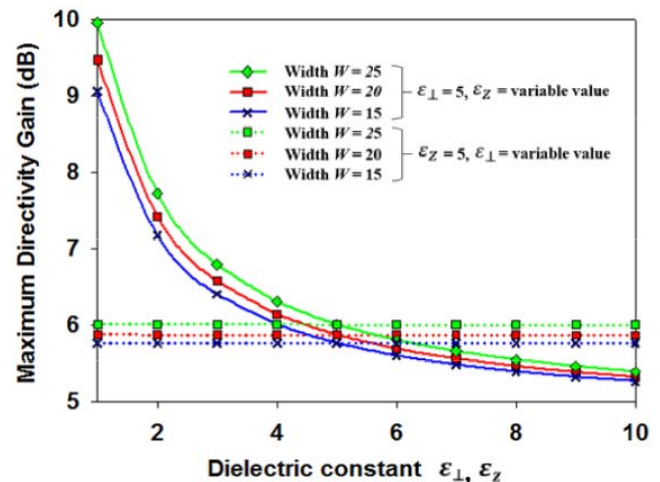


Fig. 8. Maximum directivity gain as function of anisotropic permittivity of LC.

with increasing ϵ_{\perp} , the influence of ϵ_{\perp} on the radiation pattern is insignificant. At the H-plane of TM_{030} mode, the 3-dB beamwidth of the radiation pattern increases with increasing ϵ_z , but ϵ_{\perp} cannot influence the radiation pattern much.

Fig. 8 shows the calculated results of the maximum directivity according to the permittivity tensor properties where the length of patch and height of substrate that are 15 and 0.51 mm, respectively. As ϵ_z increases, the maximum directivity decreases. The patch antenna on the LC substrate has a possibility to have a higher realized gain when the voltage increases, because ϵ_z increases with the rise of voltage. However, as shown in (14), the realized gain is a multiplication of directivity and radiation efficiency and is hard to predict, because the radiation efficiency is an unforeseeable factor. The effect of ϵ_{\perp} is very slight and can be neglected. In addition, as patch size increases, the maximum directivity increases.

Based on the given physical dimensions of [12], the calculated normalized radiation patterns of the patch antenna on the LC substrate are compared with the results of [12], as shown in Fig. 9. The calculated results well agree with the results of [12]. Because the calculation uses an infinite size ground plane, the trivial discrepancy at the E-plane exists between the calculated results and simulation results of [12]. However, the calculated results of the H-plane well correspond to the results of [12]. As expected, with the increase of the bias, the 3-dB beamwidth increases.

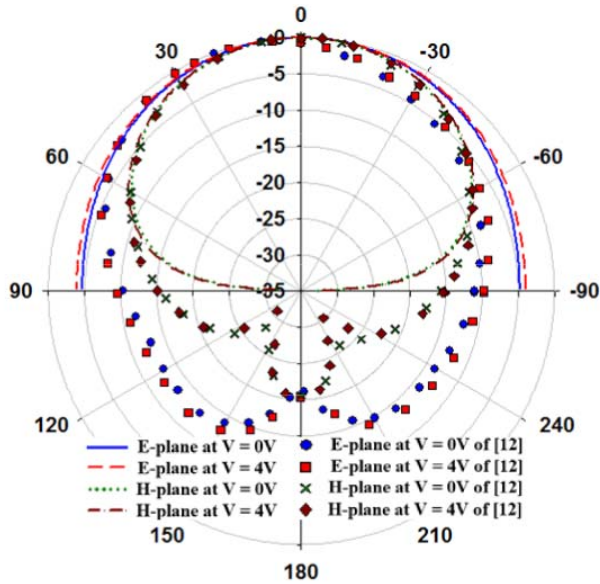


Fig. 9. Comparison of the measured results of [12] and proposed results of radiation patterns depending on the bias strength at resonance.

The radiation efficiency except for the reflection efficiency is already calculated in [12]. The radiation efficiency at 0 and 10 V are 21% and 28%, respectively. The reason why the radiation efficiency increases as the bias voltage increases is due to diminish of loss tangent of the LC that is reduced from 0.12 to 0.02. The calculated maximum directivities of (13) at 0 and 10 V are 7.0857 and 6.6648 dB, respectively. Using (14), the corresponding realized gain is 0.5 and 1.15 dB, respectively. Although the maximum directivity of biased state is lower than that of no biased state, realized gain increases due to the radiation efficiency. The broadside realized gain of [12] at 0 and 10 V is 0.7 and 1.1 dB, respectively. The calculated results well coincide with the results of [12]. As a result, it is verified that the proposed model can be the reasonable model to predict the performance of patch antenna on the LC substrate.

V. CONCLUSION

An accurate theoretical model for the resonant frequency and radiation performance of the rectangular patch antenna on the LC substrate has been introduced and verified. The effect of the permittivity tensor of the LC substrate to the resonant frequency was analyzed. The tensor component ε_z dominantly affects the resonant frequency, compared with ε_{\perp} . When ε_z increases, the resonant frequency decreases. The influence of ε_{\perp} on the resonant frequency is slight. However, as the height of the substrate increases, the influence of ε_{\perp} on the resonant frequency increases since effective height changes depending on ε_{\perp} . The proposed model was compared with the reported measured and simulation results of the patch antenna on the LC substrate. We confirmed that the calculated results of the proposed model were in a good agreement with the reported results. The maximum error between the calculated results and reported simulation results is less than 2.8%.

The effect of the properties of the anisotropic substrate to radiation pattern and maximum directivity was studied. When ε_z increases, the 3-dB beamwidth become wider and directivity decreases. The calculated results of the radiation pattern and realized gain match the reported results well. Based on the results, the proposed formula is indeed reasonable enough to derive the resonant frequency, radiation pattern, and directivity gain of the patch antenna on the LC substrate.

REFERENCES

- [1] S. Bulja, D. Mirshekar-Syahkal, R. James, S. E. Day, and F. A. Fernandez, "Measurement of dielectric properties of nematic liquid crystals at millimeter wavelength," *IEEE Trans. Microw. Theory Techn.*, vol. 58, no. 12, pp. 3493–3501, Dec. 2010.
- [2] F. Yang and J. R. Sambles, "Determination of the permittivity of nematic liquid crystals in the microwave region," *Liq. Cryst.*, vol. 30, no. 5, pp. 599–602, 2003.
- [3] L. Liu and R. J. Langley, "Liquid crystal tunable microstrip patch antenna," *Electron. Lett.*, vol. 44, no. 20, pp. 1179–1180, Sep. 2008.
- [4] N. Martin, P. Laurent, C. Person, P. Gelin, and F. Huret, "Patch antenna adjustable in frequency using liquid crystal," in *Proc. 33rd Eur. Microw. Conf.*, vol. 2, Oct. 2003, pp. 699–702.
- [5] N. Martin, P. Laurent, C. Person, P. Gelin, and F. Huret, "Size reduction of a liquid crystal-based, frequency-adjustable patch antenna," in *Proc. 34th Eur. Microw. Conf.*, Amsterdam, The Netherlands, Oct. 2004, pp. 825–828.
- [6] J.-W. Dai, H.-L. Peng, Y.-P. Zhang, and J.-F. Mao, "A novel tunable microstrip patch antenna using liquid crystal," *Prog. Electromagn. Res. C*, vol. 71, pp. 101–109, 2017.
- [7] P. Yaghmaee, C. Fumeaux, B. Bates, A. Manabe, O. H. Karabey, and R. Jakoby, "Frequency tunable S-band resonator using nematic liquid crystal," *Electron. Lett.*, vol. 48, no. 13, pp. 798–800, Jun. 2012.
- [8] S. Missaoui, S. Missaoui, and M. Kaddour, "Tunable microstrip patch antenna based on liquid crystals," in *Proc. 21st Int. Seminar/Workshop Direct Invers Problems Electromagn. Acoust. Wave Theory (DIPED)*, Sep. 2016, pp. 88–91.
- [9] R. Bose and A. Sinha, "Tunable patch antenna using a liquid crystal substrate," in *Proc. IEEE Radar Conf.*, May 2008, pp. 1–6.
- [10] W. C. Chew and Q. Liu, "Resonance frequency of a rectangular microstrip patch," *IEEE Trans. Antennas Propag.*, vol. AP-36, no. 8, pp. 1045–1056, Aug. 1988.
- [11] F. Bouttout, F. Benabdelaziz, A. Benghalia, D. Khedrouch, and T. Fortaki, "Uniaxially anisotropic substrate effects on resonance of rectangular microstrip patch antenna," *Electron. Lett.*, vol. 35, no. 4, pp. 255–256, Feb. 1999.
- [12] A. C. Polycarpou, M. A. Christou, and N. C. Papanicolaou, "Tunable patch antenna printed on a biased nematic liquid crystal cell," *IEEE Trans. Antennas Propag.*, vol. 62, no. 10, pp. 4980–4987, Oct. 2014.
- [13] C. A. Balanis, *Antenna Theory: Analysis and Design*, 3rd ed. Hoboken, NJ, USA: Wiley, 2005.
- [14] P. Yaghmaee, O. H. Karabey, B. Bates, C. Fumeaux, and R. Jakoby, "Electrically tuned microwave devices using liquid crystal technology," *Int. J. Antennas Propag.*, vol. 2013, Sep. 2013, Art. no. 824214.
- [15] K. Hirasawa and M. Haneishi, Eds., *Analysis, Design and Measurement of Small and Low-profile Antennas*. Dedham, MA, USA: Artech House, 1992.
- [16] M. V. Schneider, "Microstrip lines for microwave integrated circuits," *Bell Syst. Tech. J.*, vol. 48, no. 5, pp. 1421–1444, May/June 1969.
- [17] G. Perez-Palomino, J. A. Encinar, and M. Barba, "Accurate electromagnetic modeling of liquid crystal cells for reconfigurable reflectarrays," in *Proc. 5th Eur. Conf. Antennas Propag.*, Rome, Italy, Apr. 2011, pp. 997–1001.
- [18] R. M. Nelson, D. A. Rogers, and A. G. D'Assuncao, "Resonant frequency of a rectangular microstrip patch on several uniaxial substrates," *IEEE Trans. Antennas Propag.*, vol. 38, no. 7, pp. 973–981, Jul. 1990.
- [19] K.-L. Wong, J.-S. Row, C.-W. Kuo, and K.-C. Huang, "Resonance of a rectangular microstrip patch on a uniaxial substrate," *IEEE Trans. Microw. Theory Techn.*, vol. 41, no. 4, pp. 698–701, Apr. 1993.



Tae-Wan Kim was born in Masan, South Korea, in 1988. He received the B.S. degree from the University of Konkuk, Seoul, South Korea, in 2013, the M.S. degree in electrical engineering from the Korea Advanced Institute of Science and Technology, Daejeon, South Korea, in 2015, where he is currently pursuing the Ph.D. degree in electrical engineering.

His current research interests include ferrite loaded antennas and material measurement.



Jun-Sung Park was born in Daegu, South Korea, in 1993. He received the B.S. degree from Kyungpook National University, Daegu, in 2017. He is currently pursuing the M.S. degree in electrical engineering with the Korea Advanced Institute of Science and Technology, Daejeon, South Korea.

His current research interests include ferrite loaded antennas and dielectric resonator antenna.



Seong-Ook Park (M'05–SM'11) was born in Yeongcheon, South Korea, in 1964. He received the B.S. degree from KyungPook National University, Daegu, South Korea, in 1987, the M.S. degree from the Korea Advanced Institute of Science and Technology, Daejeon, South Korea, in 1989, and the Ph.D. degree from Arizona State University, Tempe, AZ, USA, in 1997, all in electrical engineering.

From 1989 to 1993, he was a Research Engineer with Korea Telecom, Daejeon, where he was involved in microwave systems and networks. He joined the Telecommunication Research Center, Arizona State University, until 1997. Since 1997, he has been with Information and Communications University, Daejeon, as an Associate Professor, where he is currently a Professor with the Korea Advanced Institute of Science and Technology. His current research interests include mobile handset antenna and analytical and numerical techniques in the area of electromagnetics.

Dr. Park is a member of Phi Kappa Phi.